Atypical molecular basis for drug resistance to mitochondrial function inhibitors in *Plasmodium falciparum*

Heather J. Painter[1,a], Joanne M. Morrisey[2], Michael W. Mather[2], Lindsey M. Orchard[1], Cuyler Luck[1], Martin J. Smilkstein[3], Michael K. Riscoe[3], Akhil B. Vaidya[2], Manuel Llinás[1]

[1] Department of Biochemistry and Molecular Biology, Huck Center for Malaria Research, Pennsylvania State University, University Park, PA, USA

[2] Center for Molecular Parasitology, Department of Microbiology and Immunology, Drexel University College of Medicine, Philadelphia, PA, USA

[4] Medical Research Service, Department of Veterans Affairs Medical Center, Portland, OR, USA

[a] Current affiliation: United States Food & Drug Administration, Center for Biologics & Evaluation Research, Office of Vaccine Research & Review, Division of Parasites, Bacteria & Allergenic Products, Silver Spring, MD, USA

[#] Corresponding authors: manuel@psu.edu and Heather.Painter@fda.hhs.gov

Abstract:

The continued emergence of drug-resistant *Plasmodium falciparum* parasites hinders global attempts to eradicate malaria, emphasizing the need to identify new antimalarial drugs. Attractive targets for chemotherapeutic intervention are the cytochrome (cyt) bc_1 complex, which is an essential component of the mitochondrial electron transport chain (mtETC) necessary for ubiquinone recycling and mitochondrially localized dihydroorotate dehydrogenase (DHODH) critical for *de novo* pyrimidine synthesis. Despite the essentiality of this complex, resistance to a novel acridone class of compounds targeting cyt bc_1 was readily attained, resulting in a parasite strain (SB1-A6) that was pan-resistant to both mtETC and DHODH inhibitors. Here we describe the molecular mechanism behind the resistance of the SB1-A6 parasite line which lacks the common cyt bc_1 point mutations characteristic of resistance to mtETC inhibitors. Using Illumina whole-genome sequencing, we have identified both a copy number variation (~2x) and a single-nucleotide polymorphism (C276F) associated with *pfdhodh* in SB1-A6. We have characterized the role of both genetic lesions by mimicking the copy number variation via episomal expression of *pfdhodh* and introducing the identified SNP using CRISPR/Cas9 and assessed their contributions to drug resistance. Although both of these genetic polymorphisms have been previously identified as contributing to both DSM-1 (1) and atovaquone resistance (2, 3), SB1-A6 represents a unique genotype in which both alterations are present in a single line, suggesting that the combination contributes to the pan-resistant phenotype. This novel mechanism of resistance to mtETC inhibition has critical implications for the development of future drugs targeting the bc_1 complex or *de novo* pyrimidine synthesis that could help guide future anti-malarial combination therapies and reduce the rapid development of drug resistance in the field.

43 **Introduction:**

44 Infection by the human malaria parasite *Plasmodium falciparum* rapidly leads to the clinical
45 symptoms associated with the 48-hour asexual replicative cycle of the parasite within the blood of
46 the host (4). *P. falciparum* malaria continues to present an enormous global public health burden
47 due to the lack of an effective long-term vaccine (5) and the emergence of resistance to front-line
48 antimalarial chemotherapies (6). This underscores the continued need to maintain a robust drug
49 development pipeline that produces novel and effective antimalarial compounds for future
50 deployment.

51 To accelerate novel anti-malarial compound identification, independent laboratories and global
52 consortia have rapidly identified numerous chemical entities that are efficacious against multiple
53 *Plasmodium* species and developmental stages. Despite the diverse chemical scaffolds in the
54 compounds tested, most effective candidates tend to have similar modes-of-action in the malaria
55 parasite due to the paucity of molecular targets that are significantly divergent from the human
56 host (7-9). As such, it is not surprising that a large and diverse set of compounds selectively target
57 the highly divergent *Plasmodium* mitochondrion (7), which is essential for *de novo* pyrimidine
58 synthesis during the blood stages of parasite development (10, 11).

59 Although the *Plasmodium* mitochondrion maintains the canonical tricarboxylic acid cycle pathway
60 of central carbon metabolism (12-15), these enzymes are dispensable for blood-stage development
61 (15). We have previously shown the main role of the parasite mitochondrion during the blood-
62 stage is the provision of precursors for *de novo* pyrimidine synthesis (10), a process requiring a
63 ubiquinone-dependent, mitochondrional dihydroorotate dehydrogenase (DHODH,
64 PF3D7_0603300) and a functioning electron transport chain (ETC) to maintain turnover of

65 ubiquinol, regenerating ubiquinone. This sole essential function of the mitochondrion was
66 established by genetic supplementation with an alternative DHODH from *S. cerevisiae*
67 (yDHODH), which is localized to the cytoplasm and utilizes fumarate as an electron acceptor
68 rather than ubiquinone (10). Therefore, parasites expressing yDHODH from an episome,
69 bypassing the mitochondrially localized PfDHODH, are highly resistant to all chemical inhibitors
70 of the mtETC. Interestingly, the addition of the biguanide prodrug proguanil, combined with the
71 mtETC cytochrome *b* inhibitor atovaquone in the antimalarial drug Malarone, reversed the pan-
72 resistant phenotype of yDHODH expressing *P. falciparum* strain D10 (D10::yDHODH) (10).
73 Although the mode-of-action of atovaquone, as well as other mtETC inhibitors, is well-understood,
74 the molecular target of proguanil remains unknown.

75 Due to the efficacy of disrupting mitochondrial function in the malaria parasite as a strategy for
76 chemotherapeutic intervention, these pathways are the focus of comprehensive anti-mitochondrial
77 drug development programs, and significant efforts have been made to identify novel compounds
78 that target the mtETC both directly (cytochrome *b*) and indirectly (DHODH). To this end, there
79 are several antimalarials, some of which are in the advanced stages of clinical trials, whose
80 proposed modes-of action include interaction with the ubiquinone binding pocket(s) of DHODH
81 (DSM-1 and DSM265) (16-18) or cytochrome *b* (ELQ-300 and 6-NH_2Ac) (19, 20). Despite the
82 essentiality of both components of the mtETC, resistance to these compounds readily arose and
83 genotyping of resistant parasites revealed either amplification of or point mutations in DHODH,
84 as well as point mutations within cytochrome *b* (1, 2, 16, 21-23). However, parasites resistant to
85 6-NH_2Ac, an acridone compound thought to target the mtETC bc_1 complex (20), did not exhibit
86 traditional bc_1 resistance mutations (21). The acridone-resistant parasite line SB1-A6 was not only
87 resistant to 6-NH_2Ac but also exhibited pan-resistance to all mitochondrial inhibitors to which the

88 parent strain, D6, was susceptible (21). Again, this resistance was abrogated by the addition of
89 proguanil (21), similar to *P. falciparum* parasites that express yDHODH, and confirming the target
90 of acridones to be the *P. falciparum* mtETC, although the provenance of the phenotypic similarities
91 in resistance to bc_1 complex inhibitors between SB1-A6 and the yDHODH transgenic parasite line
92 was unclear (10).

93 In this study, we present a clear genotype for the *P. falciparum* SB1-A6 acridone-resistant clonal
94 parasite strain and, through a combination of targeted and whole-cell methods, establish that the
95 mechanism of resistance to both cytochrome bc_1 and DHODH inhibitors results from the
96 contribution of multiple genetic polymorphisms. We find that *P. falciparum* SB1-A6 accumulates
97 both a copy number variation and a specific mutation in PfDHODH, and both of these genetic
98 polymorphisms contribute to the pan-resistant phenotype. This study uncovers a mechanism of
99 cross-resistance between PfDHODH and mtETC inhibitors and serves as a cautionary note to
100 future anti-malarial combination therapy formulations containing such drugs.

101

102 **Results:**

103 **Strain SB1-A6 displays pan-resistance to mtETC inhibitors.**

104 To confirm the resistance phenotype of *P. falciparum* SB1-A6 (21) and the line's similarity to *P.*
105 *falciparum* D10::yDHODH (10), we first tested the susceptibility of both strains to the classic
106 malaria parasite cytochrome bc_1 inhibitor, atovaquone, using a growth inhibition assay (Fig. 1A,
107 Table S1). As expected, both SB1-A6 and D10::yDHODH displayed resistance to atovaquone,
108 while the parental strains (D6 and D10, respectively) were susceptible (Fig. 1A. Table S1), as
109 previously published (21). It has been well established that expression of yDHODH in *P.*

110 *falciparum* results in resistance to the PfDHODH inhibitor DSM-1 (24, 25). Therefore, we tested
111 the susceptibility of SB1-A6 to direct inhibition of PfDHODH with DSM-1 (17) and found that
112 this parasite line was resistant to both DHODH, as well as cytochrome bc_1 inhibitors (Figure 1B,
113 Table S1), making it the first *P. falciparum* clone generated to exhibit such cross-resistance (21).
114 However, more recent studies aimed at generating resistance to atovaquone by increasing drug
115 concentration exposure step-wise have also resulted in cross-resistance to DSM-1 (2). Resistance
116 to mtETC inhibitors due to an alternative source of pyrimidines is abolished by the addition of the
117 prodrug proguanil (10). Likewise, resistance to atovaquone inhibition of the mtETC in SB1-A6
118 was reversed upon the addition of 1.5µM proguanil (Fig. 1B, Table S1), suggesting that the
119 mechanism of pan-resistance to mitochondrial inhibitors is linked to the function of PfDHODH,
120 as was previously demonstrated for D10::yDHODH (10).

121 Drug resistance mechanisms in both prokaryotes and eukaryotes can involve "rewiring" to
122 overcome the inhibition of essential metabolic pathways by genetic variation, metabolic bypass,
123 or efflux mechanisms. Metabolomics has become a useful tool for unraveling anti-parasite drug
124 mechanisms of action and resistance (8, 26, 27). To elucidate the mechanism(s) of resistance in
125 SB1-A6, we determined if any metabolic perturbations occurred in the SB1-A6 drug-resistant line
126 due to drug treatment that could account for cross-resistance to both PfDHODH and cytochrome
127 bc_1 inhibition, using whole-cell metabolomics analysis. Trophozoite-stage D6 and SB1-A6 were
128 exposed to ~10x IC50 of either atovaquone (10nM) or DSM-1 (1.5µM) for 2 hours, followed by
129 whole-cell metabolite extraction, and quantitated by LC-MS/MS analysis (8). Metabolomic
130 analysis showed that treatment of SB1-A6 with DSM-1 or atovaquone did not result in any
131 significant metabolic perturbation (Fig. 1C and 1D; Table S1), whereas treatment of the wild-type
132 D6 revealed an accumulation of *de novo* pyrimidine synthesis precursors compared to an untreated

133 control (Fig 1C and 1D). The accumulation of pyrimidine precursors in the parental line upon
134 treatment with either atovaquone or DSM-1 and lack of accumulation in the treated mutant line
135 (Fig. 1D), in neither a stage- nor time-dependent manner (Fig. S1) is consistent with the
136 involvement of DHODH in the mechanism of resistance.

137 **Genetic determinants of pan-resistance to mtETC and pyrimidine synthesis inhibition in**
138 **SB1-A6.**

139 Previous studies have demonstrated that genetic mechanisms of resistance resulting in the ability
140 of the parasite to overcome mtETC and *de novo* pyrimidine synthesis inhibition include mutations
141 in either *cytochrome b* (28, 29) or *pfdhodh* (1, 30) or copy number variation of *pfdhodh* (2, 3).
142 Analysis of the SB1-A6 *cytochrome b* sequence by Smilkstein *et al.* (21) did not reveal any
143 mutations. Therefore, to identify any genetic polymorphisms that could lead to a molecular
144 mechanism of resistance, we examined the genomes of both the D6 wild-type and SB1-A6 drug-
145 resistant parasites using Illumina-based next-generation DNA sequencing. Whole-genome
146 sequencing revealed a non-synonymous G → T point-mutation in the coding sequence of
147 PfDHODH, resulting in the amino acid change C276F (Fig. 2A, Table S2). Amino acid C276 is
148 localized adjacent to the flavin mononucleotide binding pocket (Fig. 2C), and the substitution to a
149 phenylalanine has been demonstrated to reduce the size of the binding pocket where DSM-1 binds
150 (1), resulting in a binding pocket structure resembling that of HsDHODH (30). Although this
151 mutation was not the only change found in SB1-A6 (Table S2), it was the only change in an
152 annotated gene known to be directly linked to pyrimidine synthesis and/or mitochondrial function.

153 In addition, we identified a ~20kb, 2-fold copy number variation (CNV) in the SB1-A6 genome,
154 including the coding sequence for PfDHODH, as well as six other protein-coding genes (Fig. 2B).
155 We further confirmed the presence of this copy number increase by DNA microarray comparative

156 genome hybridization (Table S3). This region has previously been shown to increase in copy
157 number in *P. falciparum* selected for resistance to DSM-1 (3), resulting in cross-resistance to
158 atovaquone (2). Although each of these genetic polymorphisms has individually been previously
159 identified as contributing significantly to both DSM-1 (1) and atovaquone resistance (2, 3), SB1-
160 A6 possesses a unique genotype in which both alterations are present in a single parasite line,
161 suggesting that the combination contributes to the pan-resistant phenotype of this line.
162 Intriguingly, the increased CNV of PfDHODH did not directly translate to higher protein levels
163 (Fig. 2D), nor did it produce any obvious mislocalization (Fig. S2) of the protein in the parasite.

164 Due to previous observations that linked the PfDHODH C276F mutation and CNV to both DSM-
165 1 and atovaquone resistance, respectively (2, 3), we examined the function of PfDHODH in
166 mitochondria isolated from D6 and SB1-A6 to determine if these polymorphisms could account
167 for the reduced sensitivity of SB1-A6 parasites to mitochondrial inhibition. Measurement of
168 DHODH activity in isolated mitochondria from trophozoite stages of D6 and SB1-A6 revealed
169 that the enzymes of both strains are equally susceptible to inhibition by DSM-1 (Fig. 2E),
170 confirming the results from purified wild-type and C276F mutant PfDHODH activity assays (1).
171 Interestingly, measurement of the specific activity of DHODH from SB1-A6 isolated mitochondria
172 revealed a two-fold increase compared to D6 (Fig. 2F), possibly due to the increase in copy number
173 of PfDHODH. Although the C276F mutation does not lead to a decrease in the ability of DSM-1
174 to inhibit PfDHODH, these data suggest that the SB1-A6 parasite line has gained the ability to
175 withstand either mtETC or pyrimidine biosynthesis inhibition by increasing the overall activity of
176 PfDHODH allowing sufficient levels of nucleotide synthesis for parasite survival.

177 **Genetic supplementation of DHODH increase copy number and CRISPR-Cas9 introduction**
178 **of C276F point mutation**

179 Previous studies have established that *P. falciparum* grown in the presence of step-wise increasing
180 concentrations of DSM-1 leads to an increase in copy number of a chromosomal region that
181 includes PfDHODH leading to resistance to both DSM-1 (3) and atovaquone (2). To test the
182 hypothesis that a copy number increase in PfDHODH also results in decreased sensitivity of SB1-
183 A6 parasites to inhibition of electron transport or *de novo* pyrimidine synthesis, we introduced
184 either wild-type or mutant (C276F) PfDHODH expressed from an episomal vector under the
185 control of a constitutive promoter in the drug-susceptible strain D6 (Fig. 3A). After selection of a
186 parasite population containing the mutant or wild-type PfDHODH, we assessed the susceptibility
187 of these parasites to atovaquone or DSM-1 using a standard growth inhibition assay. The
188 introduction of additional copies of PfDHODH resulted in decreased susceptibility to DSM-1 and
189 atovaquone (Fig. 3B). Notably, the episomal expression of the mutant PfDHODH also results in
190 almost complete resistance to atovaquone (Fig. 3B), phenocopying the genotype of SB1-A6.
191 Episomal increase of wild-type PfDHODH results in a ten to 100-fold decrease in susceptibility to
192 DSM-1 (Fig. 3B), confirming the phenotype established by Guler *et al.* of DSM-1 and atovaquone
193 resistant parasites with an increased copy number of PfDHODH (2, 3).

194 Since the discovery that *P. falciparum* survival is dependent upon *de novo* pyrimidine synthesis
195 (10), PfDHODH has become a popular target for chemical intervention strategies (17, 18, 31, 32).
196 For example, discovery efforts have led to the development of triazolopyrimidine-based inhibitors
197 for PfDHODH, which are currently undergoing clinical trials for safety and efficacy (16, 33). *In*
198 *vitro* selection of *P. falciparum* for resistance to compound DSM265 led to the identification of
199 various mutations within PfDHODH (1). Of these mutations, C276F was determined to reduce
200 the binding capacity of chemical inhibitors using in an *in vitro* expression system (1), as well as
201 computational docking studies (30). To test the hypothesis that the same observed point mutation

202 in SB1-A6 PfDHODH contributes to *P. falciparum* resistance to both PfDHODH and cytochrome
203 bc_1 inhibitors, we utilized CRISPR/Cas9 (34) to genetically introduce the C276F mutations into
204 this gene in D6 and also repair it in SB1-A6 (Fig. 3C; Fig S3A and S3B). After confirming the
205 introduction or repair of the mutation at amino acid 276 (Fig. S3A and S3B), we then performed
206 drug susceptibility assays to quantitate the contribution of this mutation to the pan-resistant
207 phenotype (Table S1). While we were able to reverse this mutation to the wild-type background
208 in $A6^{F276C}$ decreasing the overall resistance to both atovaquone and DSM-1 (Fig. 3D, Table S1),
209 there remains an increased CNV of PfDHODH, which is likely contributing to the higher IC50
210 than demonstrated for D6 (Fig. 3D; Table S1). Conversely, susceptibility to atovaquone is only
211 decreased by 2-fold due to the introduction of C276F into strain D6 (Fig. 3D; Table S1).
212 Interestingly, these assays show that this mutation results in a 10-fold increase in the IC50 of DSM-
213 1 in $D6^{C276F}$ (Fig. 3D) and a 40-fold decrease in $A6^{F276C}$ (Fig. 3D). These results suggest that the
214 point mutation directly contributes to decreased efficacy of direct inhibition of PfDHODH and
215 enhances the ability of *P. falciparum* to overcome mtETC inhibition (Table S1). Taken together,
216 these data demonstrate the coordination between genetic polymorphisms of the PfDHODH SNP
217 and CNV in the SB1-A6 parasite line that mediates the pan-resistance phenotype.

218 **Discussion:**

219 In this study, we have demonstrated the coordination of two genetic polymorphisms that result in
220 resistance to compounds that target the mtETC. First, the copy number increase of DHODH results
221 in the reduced susceptibility to bc_1 complex and *de novo* pyrimidine synthesis inhibition.
222 However, a two-fold increase in DHODH, by itself, was not sufficient for complete resistance to
223 mtETC inhibitors, potentially due to a reliance on other genes within the CNV amplicon. Aside
224 from DHODH, this amplicon encompasses seven genes, a majority of which are unannotated,

225 except for PF3D7_0603200 (*bcs1*: mitochondrial chaperone, putative) and PF3D7_0602800 (*jmjc*:
226 jumanji-C demethylase domain containing), the gene products of which could contribute to the
227 drug-resistant phenotype. This is supported by previous studies that demonstrated that a similar
228 amplicon results in resistance to both atovaquone and DSM-1 (2, 3). Further work is necessary to
229 determine if the proteins encoded for on the amplicon are involved in reducing the parasite's
230 susceptibility to mtETC and *de novo* pyrimidine synthesis inhibition.

231 The implications of the SB1-A6 phenotype raises serious questions into the continued viability of
232 the cytochrome bc_1 complex as an anti-malarial drug target. While the adaptation that led to SB1-
233 A6 seems to have been a unique event, both the CNV and C276F point mutations have each been
234 derived independently from exposure to atovaquone and DSM-256, a next-generation PfDHODH
235 inhibitor currently in clinical trials. Therefore, the possibility that adaptations similar to those
236 found in SB1-A6 may arise during clinical trials or deployment of new bc_1 complex or DHODH
237 inhibitors deserves consideration. While concerns regarding atovaquone resistant mutations in the
238 *cytb* gene on mtDNA have been largely allayed due to lack of inheritance during transmission
239 within the mosquito vector (35), we have no reason to discount the transmissibility of nuclear-
240 encoded *pfdhodh* polymorphisms at present. Since these adaptations can be overcome by the
241 addition of proguanil, future combination therapies should continue to consider formulations that
242 include this prodrug.

243 This study presents the first identification of the acquisition of multiple genetic polymorphisms in
244 response to a bc_1 complex inhibitor that results in pan-resistance to both direct and indirect
245 inhibitors of DHODH. Fully elucidating the molecular mechanisms of this pan-resistance is
246 essential to inform future chemotherapeutic targeting strategies for malaria elimination. The
247 emergence of resistance to many of the drugs in the antimalarial arsenal has highlighted the

248 urgency of developing future medicines with modes of action distinct to those of the current
249 therapies. More recently, considerations have been made for combination therapies that target a
250 single essential metabolic pathway via different modes-of-action. In light of the potential
251 development of cross-resistance to a single inhibitor due to its combinatorial partner, the molecular
252 mechanisms of resistance for future therapeutic strategies should be thoroughly investigated prior
253 to approval for use in the clinical setting.

254 Recently, the essentiality of DHODH has been demonstrated in cell-cycle arrested cancer cells
255 without mitochondria wherein reactivation of growth occurs upon the acquisition of mtETC-linked
256 DHODH (36), suggesting that the lack of de novo pyrimidine synthesis is a major obstacle for in
257 vivo growth of respiration-compromised tumor cells. The combined detrimental effects of both
258 dysfunctional mitochondrial respiration and mtETC-linked de novo pyrimidine synthesis on cell
259 growth strengthen their relevance as drug targets against both parasite development and
260 metastatic cell growth. This further emphasizes the continued benefit of identifying novel
261 inhibitors of DHODH that could ultimately be appropriated for both parasite elimination and
262 perhaps extended to treatment targeting metastatic cells within the human host.

263

264 **Methods:**

265 ***Parasite Strains and Culture:*** *Plasmodium falciparum* strains D6 and SB1-A6 were provided by
266 Michael Riscoe and Martin Smilkstein (21). All parasites obtained from other sources or generated
267 in this study were maintained under standard conditions (37) at 2% hematocrit with O+ human
268 erythrocytes in RPMI1640 (Thermo Fisher Scientific) containing hypoxanthine, NaH_2CO_3
269 (Sigma-Aldrich), HEPES (Sigma-Aldrich), glutamine (Sigma-Aldrich) and 2.5 g/L AlbuMAX II

270 (Thermo Fisher Scientific). Intraerythrocytic developing parasites were synchronized with 5%
271 sorbitol (Sigma-Aldrich) over three subsequent developmental cycles to synchronize parasites
272 within 4-6 hours, as previously described (38).

273 Parasite cultures were maintained Mycoplasma-free and were confirmed prior to metabolomic
274 analysis. Separate mycoplasma-free culture apparatus and solutions were used for all
275 metabolomics culturing to prevent contamination. Cultures were checked for mycoplasma
276 contamination weekly using IntronBio *e*-Myco™, Mycoplasma PCR Detection kit (Boca
277 Scientific; cat. no. 25235). If parasite cultures tested positive for Mycoplasma, cultures were
278 treated as per manufacturer's instructions with Mycoplasma Removal Agent (MP Biomedicals,
279 LLC.; cat. no. 30-500-44).

280

281 ***Drug Inhibition Assays:*** All parasite growth inhibition assays were performed in 96-well plates
282 as described by Desjardin *et al.* (39) and adapted for SYBR Green I (40). Drugs were prepared in
283 DMSO as a 500× dilution series (typically a 2- or 3-fold dilution series was used, yielding a final
284 concentration in media ranging from 0.001−30 μM depending on the cell line) and were then
285 diluted 1:50 into media to yield a final DMSO concentration of 0.2%. Parasites were diluted to 1%
286 parasitemia and 1% hematocrit in each well of a 96-well plate then propagated for 48 h and growth
287 was assessed using the SYBR Green method. SYBR green fluorescence was measured (ex./em.
288 485/535 nm) and data analysis was performed using GraphPad Prism 7. For transgenic *P.*
289 *falciparum* strains generated in this study, parasites were propagated for three intraerythrocytic
290 cycles in media lacking drug before plating. All data were collected in triplicate and biological
291 duplicate.

292

293 ***Mitochondrial Activity Assays:*** *P. falciparum* cultures were synchronized at least twice by
294 treatment with alanine (41), expanded and harvested at 8-15% parasitemia in the mid to late
295 trophozoite stages. A hemozoin-depleted mitochondrial fraction was isolated from the parasites
296 using nitrogen cavitation, magnetic separation, and differential centrifugation, as previously
297 described (42).

298 DHODH activity assays were conducted essentially as previously described (18, 42) with minor
299 modifications, utilizing the ubiquinone analog decylubiquinone as the primary electron acceptor,
300 coupled to the redox dye 2,6-dichloroindophenol to take advantage of the latter's higher extinction
301 coefficient and absorbance in the visible range. Assays contained 1 mM L-dihydroorotate, 100 µM
302 decylubiquinone, 60 µM 2,6-dichloroindophenol, 50 mM sodium malonate, 2 mM potassium
303 cyanide, 100 mM potassium chloride, 0.05% Triton X-100, 10 % glycerol, and 0.1 M HEPES (pH
304 7.6) in a final volume of 1 ml. 5 ul aliquots of diluted inhibitor or vehicle (DMSO) was added, and
305 each assay was initiated by addition of a 7 µl aliquot of mitochondrial preparation (50-110 µg
306 protein) and recorded with a modified SLM-AMINCO DW2C dual-wavelength
307 spectrophotometer (On-Line Instrument Systems, Inc., Bogart, GA, USA) in dual mode (600 nm
308 – 528 nm) at 30°C.

309

310 ***Inhibitors:*** The antimalaria compound atovaquone was a gift from Glaxo Wellcome, Research
311 Triangle Park, N.C. Proguanil was kindly provided by the Jacobus Pharmaceutical Company,
312 Princeton, NJ, USA. Both ELQ-300 and 6-NH2Ac were contributed to this study by Michael
313 Riscoe, Oregon Health Sciences University, Portland, OR, USA. DSM-1 (17) and DSM-265 (16)

314 were provided by Margaret Phillips, University of Texas Southwestern, Dallas, TX, USA.
315 Chloroquine (Cat# C6628) was purchased from Sigma-Aldrich, St. Louis, MO, USA.

316

317 ***Whole-cell Metabolomics:*** Metabolite extractions, data collection, and analysis were performed
318 as described previously (8, 43, 44). Briefly, a ~20 µL pellet of cells was resuspended in 1 mL of
319 pre-chilled 90:10 methanol:water and placed at 4˚C. The internal standard $^{13}C_4$-$^{15}N_1$-aspartate was
320 spiked into the extraction methanol solution to control for sample preparation and handling.
321 Samples were vortexed, resuspended, and centrifuged for 10 min at 15000 RPM and 4˚C.
322 Supernatants were collected and stored at -80˚C or dried down immediately under nitrogen flow.
323 The dried metabolites were resuspended in HPLC-grade water (Sigma-Aldrich, CHROMASOLV)
324 to between $1x10^5$ and $1x10^6$ cells/µL, based on hemocytometer counts of purified parasites. All
325 samples were processed in technical triplicate with method blanks to reduce unwanted variation
326 and account for background signal, respectively. Samples were randomized and 10µL of
327 resuspended metabolite extract or method blank was injected for ultraHigh-Performance Liquid
328 Chromatography-Mass Spectrometry (HPLC-MS) analysis.

329 Extracts were analyzed using HPLC-MS on a Thermo Exactive Plus Orbitrap™. Metabolite
330 separation was performed with a C18 column (Phenomenex Hydro-RP; cat. No 00D-4387-B0)
331 using a 25 minute gradient of A: 3% aq. methanol/15mM acetic acid/10 mM tributylamine ion-
332 pairing agent and B: 100% MeOH (45). Metabolite detection was performed using a scan range
333 of 85-1000 m/z and a resolution of 140,000 @ m/z 200, in negative ion mode. The detection of
334 cellular metabolites was aided by the generation of a database from 292 pure metabolite standards
335 using the same instrument and method to determine detection capability, mass/charge ratio (m/z),

336 and retention time for each metabolite. Analysis of data was carried out as previously described
337 (8).

338

339 ***Whole-genome Sequencing and Analysis:*** Genomic DNA was isolated, prepared from *P.*
340 *falciparum* parasite lines, and sequenced as previously described (46). Briefly, a total of 10 µg of
341 gDNA from each line was sheared to obtain a fragment size of ~200–400 bp. The resulting sheared
342 gDNA was size selected on a 2% (w/v) low-melting agarose gel and then purified and concentrated
343 using MinElute purification columns followed by the QIAquick PCR purification kit (QIAGEN).
344 Barcoded libraries for Illumina TruSeq single-end sequencing were then constructed from the size-
345 selected, sheared material and size selected using Agencourt AMPure XP magnetic beads
346 (Agencourt Biosciences, Beckman Coulter). The quality of the final sequencing libraries was
347 assessed using an Agilent 2100 Bioanalyzer (Agilent Technologies) and the concentration of each
348 library was quantified using a Quant-iT dsDNA Broad-Range Assay Kit (Invitrogen). The final
349 libraries were multiplexed and 20% (v/v) PhiX control DNA (Illumina, Catalog # FC-110-3001)
350 per lane and were sequenced using an Illumina HiSeq 2500 Rapid Run (150 bp) system (Illumina).

351

352 Sequencing outputs were uploaded into Galaxy (47), which is hosted locally at the Millennium
353 Science Complex at Pennsylvania State University. Sequence reads were mapped to the *P.*
354 *falciparum* 3D7 reference genome v. 10.0 (http://plasmodb.org/common/downloads/release-
355 10.0/Pfalciparum/), using the Burrows-Wheeler alignment tool while selecting and filtering unique
356 reads for Map Quality >30 (48). Sequence variations were detected by Freebayes (version 0.9.0.a)
357 using stringent filtering parameters based on quality and read depth (49, 50). Then SNPeff (version

358 3.3) was applied to annotate and determine the statistical significance of each variant (51). Genome
359 copy number variations were detected based upon local chromosomal read depth using CNVnator
360 (version 0.3) and annotated with Intansv (version 0.99.3) (52).

361

362 ***DHODH Western Blot Analysis:*** Total protein extracts were run on a 4-12% Bis-Tris gel
363 (ThermoFisher) in MES buffer and then transferred to a nitrocellulose membrane. After blocking
364 with 5% milk in PBS-T for 30 minutes, membranes were incubated overnight with the primary
365 antibody in 5% milk. Primary antibodies used were: 1:300 dilution of mouse anti-PfDHODH #3
366 (a kind gift from Margeret Phillips, University of Texas Southwestern) or 1/5000 mouse anti-
367 *Pf*Aldolase-HRP (Abcam, Cat #ab38905). The next day, membranes were washed three times with
368 PBS-T and incubated for two hours with the appropriate secondary antibody, then washed again.
369 The secondary antibody that was used was 1/5,000 goat anti-mouse HRP conjugate (Pierce). ECL
370 reagent (Pierce) was used to detect bound antibody.

371

372 ***DNA Constructs:*** To mutate DHODH using CRISPR-Cas9, complementary oligonucleotides
373 encoding the guide RNA were inserted into pDC2-U6A-hDHFR (kind gift of Marcus Lee) using
374 BbsI sites. A 515 bp homology region containing the mutation in PfDHODH (C276F) or the
375 wildtype sequence from either SB1-A6 or D6 was cloned into StrataClone (Agilent) and then
376 inserted using the NotI site of pDC2-U6A-hDHFR. The resulting plasmids are pDC2-C276F-
377 hDHFR and pDC2-F276C-hDHFR which were co-transfected with Cas9-BSD plasmid from Jose-
378 Juan Lopez-Rubio (34) into D6 and SB1-A6, respectively.

379

380 To introduce multiple copies of either the mutant or wild-type PfDHODH into D6 parasites, *Pf*
381 DHODH was amplified from SB1-A6 (mutant) or D6 (wild-type) genomic DNA including the
382 stop codon, cloned into StrataClone (Agilent), sequence-verified, and then inserted into pLN-
383 ENR-GFP (53) using the AvrII and BsiWI restriction sites. The resulting plasmids, pLN-
384 A6DHODH was transfected into D6 parasites.
385
386 ***Transfection of Plasmodium falciparum.*** Transfection of *P. falciparum* was performed as
387 previously described (54). Briefly, 5-7% ring stage parasite cultures were washed three times with
388 cytomix (55). The parasitized RBC pellet was resuspended to 50% hematocrit in cytomix. The
389 plasmid, isolated using a Qiagen Maxi kit and stored in 50 µg aliquots in ethanol, was centrifuged
390 down and resuspended in 100 µL Cytomix. The plasmid and 250 µL of the 50% parasitized RBC
391 suspension were combined and transferred to a 0.2 cm cuvette on ice. Electroporations were
392 carried out using a BioRad GenePulser set at 0.31kV, 960uF. The electroporated cells were
393 immediately transferred to a T-25 flask containing 0.2 ml uninfected 50% RBCs and 7 mL
394 medium. To select for parasites containing plasmid, medium containing 5 nM WR99210 or 1.5
395 µg/mL Blasticidin was added at 48 hrs post-transfection. Cultures were maintained under constant
396 5 nM WR92210 pressure, splitting weekly, until viable parasites were observed. To confirm the
397 successful mutation of PfDHODH, genomic DNA was purified using the Qiagen DNeasy Blood
398 & Tissue kit and the region of interest was PCR amplified and Sanger sequenced. Positive
399 transfectants were cloned by limiting dilution to obtain a pure population of transgenic parasites.
400
401
402

403 **Author's contributions:**

404 H.P., M.M., J.M., S.C., and C.L. designed and performed experiments and analyzed data. H.P.
405 wrote the manuscript and generated figures. M.M., M.S., and M.R. provided reagents, critical
406 comments, and edits. M.L. and A.V. designed the experiments, provided critical comments, edits,
407 and oversight.

408

409 **Acknowledgments:** We would like to thank the many people who have contributed to this project
410 including Dr. Andrew D. Patterson and Dr. Philip B. Smith of the Penn State Huck Institutes of
411 the Life Sciences Metabolomics Core Facility and Dr. Simon Cobbold previously of the Llinás lab
412 at Princeton University, for analytical expertise, technical oversight; Dr. Craig Praul of the
413 Genomics Core Facility of the Penn State Huck Institutes of the Life Sciences; and the Genomics
414 Core Facility at Princeton University and its staff, especially Donna Storton and Jessica Buckles
415 Wiggins. We also thank Dr. Meg Phillips and Dr. Pradip Rathod for sharing reagents and critical
416 comments. Lastly, we thank the many past and present members of the Llinás lab who supported
417 this project by enhancing the evaluation of data and provided critical comments.

418

419 **Funding Information:**

420 This work was supported by generous funding awarded to Manuel Llinás from the Bill and
421 Melinda Gates Foundation Grand Challenges Grant (Phase II - OPP1119049), an NIH Director's
422 New Innovators Award (1DP2OD001315-01), the Center for Quantitative Biology (P50
423 GM071508), and startup funding from the Pennsylvania State University. This work was also

424 supported by the Intramural Research Program of the Center for Biologics Evaluation and
425 Research, Food and Drug Administration funding awarded to Heather J. Painter.

426

427 **List of Supplemental Information:**

428 Supplemental Methods

429 Table S1: Drug susceptibility assays of various parasite lines

430 Fig S1: Effects of Inhibitors on pyrimidine synthesis precursors in both sensitive and resistant *P.*
431 *falciparum.*

432 Table S2: SNP analysis of the *P.f.* SB1-A6 genome

433 Table S3: Copy number analysis of the *P.f.* SB1-A6 genome

434 Fig S2: IFA of DHODH localization in D6 and SB1-A6

435 Fig S3: Sequence trace of C276F introduction or F276C repair

436

437 **References:**

438 1. White J, Dhingra SK, Deng X, El Mazouni F, Lee MCS, Afanador GA, Lawong A,
439 Tomchick DR, Ng CL, Bath J, Rathod PK, Fidock DA, Phillips MA. 2019. Identification
440 and mechanistic understanding of dihydroorotate dehydrogenase point mutations in
441 *Plasmodium falciparum* that confer in vitro resistance to the clinical candidate DSM265.
442 ACS Infect Dis 5:90-101.
443 2. Guler JL, White J, Phillips MA, Rathod PK. 2015. Atovaquone tolerance in *Plasmodium*
444 *falciparum* parasites selected for high-level resistance to a dihydroorotate dehydrogenase
445 inhibitor. Antimicrob Agents and Chemother 59:686-689.
446 3. Guler JL, Freeman DL, Ahyong V, Patrapuvich R, White J, Gujjar R, Phillips MA, DeRisi
447 J, Rathod PK. 2013. Asexual populations of the human malaria parasite, *Plasmodium*

448 *falciparum,* use a two-step genomic strategy to acquire accurate, beneficial DNA
449 amplifications. PLOS Pathogens 9:e1003375.
450 4. Miller LH, Ackerman HC, Su XZ, Wellems TE. 2013. Malaria biology and disease
451 pathogenesis: Insights for new treatments. Nat Med 19:156-67.
452 5. RTS SCTP. 2015. Efficacy and safety of RTS,S/AS01 malaria vaccine with or without a
453 booster dose in infants and children in Africa: final results of a phase 3, individually
454 randomised, controlled trial. Lancet 386:31-45.
455 6. Cui L, Lindner S, Miao J. 2015. Translational regulation during stage transitions in malaria
456 parasites. Ann N Y Acad Sci 1342:1-9.
457 7. Cowell AN, Istvan ES, Lukens AK, Gomez-Lorenzo MG, Vanaerschot M, Sakata-Kato T,
458 Flannery EL, Magistrado P, Owen E, Abraham M, LaMonte G, Painter HJ, Williams RM,
459 Franco V, Linares M, Arriaga I, Bopp S, Corey VC, Gnadig NF, Coburn-Flynn O, Reimer
460 C, Gupta P, Murithi JM, Moura PA, Fuchs O, Sasaki E, Kim SW, Teng CH, Wang LT,
461 Akidil A, Adjalley S, Willis PA, Siegel D, Tanaseichuk O, Zhong Y, Zhou Y, Llinas M,
462 Ottilie S, Gamo FJ, Lee MCS, Goldberg DE, Fidock DA, Wirth DF, Winzeler EA. 2018.
463 Mapping the malaria parasite druggable genome by using in vitro evolution and
464 chemogenomics. Science 359:191-199.
465 8. Allman EL, Painter HJ, Samra J, Carrasquilla M, Llinas M. 2016. Metabolomic profiling
466 of the malaria box reveals antimalarial target pathways. Antimicrob Agents and Chemother
467 doi:10.1128/AAC.01224-16.
468 9. Cobbold SA, Chua HH, Nijagal B, Creek DJ, Ralph SA, McConville MJ. 2016. Metabolic
469 dysregulation induced in *Plasmodium falciparum* by dihydroartemisinin and other front-
470 line antimalarial drugs. J Infect Dis 213:276-86.
471 10. Painter HJ, Morrisey JM, Mather MW, Vaidya AB. 2007. Specific role of mitochondrial
472 electron transport in blood-stage *Plasmodium falciparum*. Nature 446:88-91.
473 11. Painter HJ, Morrisey JM, Vaidya AB. 2010. Mitochondrial electron transport inhibition
474 and viability of intraerythrocytic *Plasmodium falciparum*. Antimicrob Agents and
475 Chemother 54:5281-7.
476 12. Vaidya AB, Painter HJ, Morrisey JM, Mather MW. 2008. The validity of mitochondrial
477 dehydrogenases as antimalarial drug targets. Trends in Parasitol 24:8-9.
478 13. MacRae JI, Dixon MW, Dearnley MK, Chua HH, Chambers JM, Kenny S, Bottova I,
479 Tilley L, McConville MJ. 2013. Mitochondrial metabolism of sexual and asexual blood
480 stages of the malaria parasite *Plasmodium falciparum*. BMC Biology 11:67.
481 14. Cobbold SA, Vaughan AM, Lewis IA, Painter HJ, Camargo N, Perlman DH, Fishbaugher
482 M, Healer J, Cowman AF, Kappe SH, Llinas M. 2013. Kinetic flux profiling elucidates
483 two independent acetyl-CoA biosynthetic pathways in *Plasmodium falciparum*. J Biol
484 Chem 288:36338-50.
485 15. Ke H, Lewis IA, Morrisey JM, McLean KJ, Ganesan SM, Painter HJ, Mather MW, Jacobs-
486 Lorena M, Llinas M, Vaidya AB. 2015. Genetic investigation of tricarboxylic acid
487 metabolism during the *Plasmodium falciparum* life cycle. Cell Reports 11:164-74.

488 16. Phillips MA, Lotharius J, Marsh K, White J, Dayan A, White KL, Njoroge JW, El Mazouni
489 F, Lao Y, Kokkonda S, Tomchick DR, Deng X, Laird T, Bhatia SN, March S, Ng CL,
490 Fidock DA, Wittlin S, Lafuente-Monasterio M, Benito FJ, Alonso LM, Martinez MS,
491 Jimenez-Diaz MB, Bazaga SF, Angulo-Barturen I, Haselden JN, Louttit J, Cui Y, Sridhar
492 A, Zeeman AM, Kocken C, Sauerwein R, Dechering K, Avery VM, Duffy S, Delves M,
493 Sinden R, Ruecker A, Wickham KS, Rochford R, Gahagen J, Iyer L, Riccio E, Mirsalis J,
494 Bathhurst I, Rueckle T, Ding X, Campo B, Leroy D, Rogers MJ, et al. 2015. A long-
495 duration dihydroorotate dehydrogenase inhibitor (DSM265) for prevention and treatment
496 of malaria. Science Trans Med 7:296ra111.
497 17. Phillips MA, Gujjar R, Malmquist NA, White J, El Mazouni F, Baldwin J, Rathod PK.
498 2008. Triazolopyrimidine-based dihydroorotate dehydrogenase inhibitors with potent and
499 selective activity against the malaria parasite *Plasmodium falciparum*. J Med Chem.
500 18. Baldwin J, Michnoff CH, Malmquist NA, White J, Roth MG, Rathod PK, Phillips MA.
501 2005. High-throughput screening for potent and selective inhibitors of *Plasmodium*
502 *falciparum* dihydroorotate dehydrogenase. J Biol Chem 280:21847-21853.
503 19. Nilsen A, LaCrue AN, White KL, Forquer IP, Cross RM, Marfurt J, Mather MW, Delves
504 MJ, Shackleford DM, Saenz FE, Morrisey JM, Steuten J, Mutka T, Li Y, Wirjanata G,
505 Ryan E, Duffy S, Kelly JX, Sebayang BF, Zeeman AM, Noviyanti R, Sinden RE, Kocken
506 CH, Price RN, Avery VM, Angulo-Barturen I, Jimenez-Diaz MB, Ferrer S, Herreros E,
507 Sanz LM, Gamo FJ, Bathurst I, Burrows JN, Siegl P, Guy RK, Winter RW, Vaidya AB,
508 Charman SA, Kyle DE, Manetsch R, Riscoe MK. 2013. Quinolone-3-diarylethers: a new
509 class of antimalarial drug. Sci Transl Med 5:177ra37.
510 20. Winter RW, Kelly JX, Smilkstein MJ, Dodean R, Bagby GC, Rathbun RK, Levin JI,
511 Hinrichs D, Riscoe MK. 2006. Evaluation and lead optimization of anti-malarial acridones.
512 Exp Parasitol 114:47-56.
513 21. Smilkstein MJ, Forquer I, Kanazawa A, Kelly JX, Winter RW, Hinrichs DJ, Kramer DM,
514 Riscoe MK. 2008. A drug-selected *Plasmodium falciparum* lacking the need for
515 conventional electron transport. Molec Biochem Parasitol 159:64-68.
516 22. Stickles AM, De Almeida MJ, Morrisey JM, Sheridan KA, Forquer IP, Nilsen A, Winter
517 RW, Burrows JN, Fidock DA, Vaidya AB, Riscoe MK. 2015. Subtle changes in endochin-
518 like quinolone structure alter the site of inhibition within the cytochrome *bc 1* complex of
519 *Plasmodium falciparum*. Antimicrob Agents Chemother 59:1977-1982.
520 23. Mandt REK, Lafuente-Monasterio MJ, Sakata-Kato T, Luth MR, Segura D, Pablos-
521 Tanarro A, Viera S, Magan N, Ottilie S, Winzeler EA, Lukens AK, Gamo FJ, Wirth DF.
522 2019. In vitro selection predicts malaria parasite resistance to dihydroorotate
523 dehydrogenase inhibitors in a mouse infection model. Sci Transl Med 11.
524 24. Ke H, Morrisey JM, Ganesan SM, Painter HJ, Mather MW, Vaidya AB. 2011. Variation
525 among *Plasmodium falciparum* strains in their reliance on mitochondrial electron transport
526 chain function. Eukaryotic Cell 10:1053-61.

527 25. Ganesan SM, Morrisey JM, Ke H, Painter HJ, Laroiya K, Phillips MA, Rathod PK, Mather
528 MW, Vaidya AB. 2011. Yeast dihydroorotate dehydrogenase as a new selectable marker
529 for *Plasmodium falciparum* transfection. Molec Biochem Parasitol 177:29-34.
530 26. Vincent IM, Barrett MP. 2015. Metabolomic-based strategies for anti-parasite drug
531 discovery. J Biomol Screen 20:44-55.
532 27. Creek DJ, Barrett MP. 2014. Determination of antiprotozoal drug mechanisms by
533 metabolomics approaches. Parasitol 141:83-92.
534 28. Ross LS, Gamo FJ, Lafuente-Monasterio MJ, Singh OM, Rowland P, Wiegand RC, Wirth
535 DF. 2014. In vitro resistance selections for *Plasmodium falciparum* dihydroorotate
536 dehydrogenase inhibitors give mutants with multiple point mutations in the drug-binding
537 site and altered growth. J Biol Chem 289:17980-95.
538 29. Srivastava IK, Morrisey JM, Darrouzet E, Daldal F, Vaidya AB. 1999. Resistance
539 mutations reveal the atovaquone-binding domain of cytochrome *b* in malaria parasites. Mol
540 Microbiol 33:704-11.
541 30. Bedingfield PTP, Cowen D, Acklam P, Cunningham F, Parsons MR, McConkey GA,
542 Fishwick CWG, Johnson AP. 2012. Factors Influencing the specificity of inhibitor binding
543 to the human and malaria parasite dihydroorotate dehydrogenases. J Med Chem 55:5841-
544 5850.
545 31. Munier-Lehmann H, Vidalain PO, Tangy F, Janin YL. 2013. On dihydroorotate
546 dehydrogenases and their inhibitors and uses. J Med Chem 56:3148-67.
547 32. Patel V, Booker M, Kramer M, Ross L, Celatka CA, Kennedy LM, Dvorin JD, Duraisingh
548 MT, Sliz P, Wirth DF, Clardy J. 2008. Identification and characterization of small molecule
549 inhibitors of *Plasmodium falciparum* dihydroorotate dehydrogenase. J Biol Chem
550 283:35078-35085.
551 33. Wells TNC, Van Huijsduijnen RH, Van Voorhis WC. 2015. Malaria medicines: a glass
552 half full? Nat Rev Drug Discov 14:424-442.
553 34. Ghorbal M, Gorman M, Macpherson CR, Martins RM, Scherf A, Lopez-Rubio J-J. 2014.
554 Genome editing in the human malaria parasite *Plasmodium falciparum* using the CRISPR-
555 Cas9 system. Nat Biotech 32:819-821.
556 35. Goodman CD, Siregar JE, Mollard V, Vega-Rodriguez J, Syafruddin D, Matsuoka H,
557 Matsuzaki M, Toyama T, Sturm A, Cozijnsen A, Jacobs-Lorena M, Kita K, Marzuki S,
558 McFadden GI. 2016. Parasites resistant to the antimalarial atovaquone fail to transmit by
559 mosquitoes. Science 352:349-53.
560 36. Bajzikova M, Kovarova J, Coelho AR, Boukalova S, Oh S, Rohlenova K, Svec D,
561 Hubackova S, Endaya B, Judasova K, Bezawork-Geleta A, Kluckova K, Chatre L,
562 Zobalova R, Novakova A, Vanova K, Ezrova Z, Maghzal GJ, Magalhaes Novais S,
563 Olsinova M, Krobova L, An YJ, Davidova E, Nahacka Z, Sobol M, Cunha-Oliveira T,
564 Sandoval-Acuña C, Strnad H, Zhang T, Huynh T, Serafim TL, Hozak P, Sardao VA,
565 Koopman WJH, Ricchetti M, Oliveira PJ, Kolar F, Kubista M, Truksa J, Dvorakova-
566 Hortova K, Pacak K, Gurlich R, Stocker R, Zhou Y, Berridge MV, Park S, Dong L,

567 Rohlena J, Neuzil J. 2019. Reactivation of dihydroorotate dehydrogenase-driven
568 pyrimidine biosynthesis restores tumor growth of respiration-deficient cancer cells. Cell
569 Metabol 29:399-416.e10.
570 37. Trager W, Jensen JB. 1976. Human malaria parasites in continuous culture. Science
571 193:673-5.
572 38. Lambros C, Vanderberg JP. 1979. Synchronization of *Plasmodium falciparum* erythrocytic
573 stages in culture. J Parasitol 65:418-20.
574 39. Desjardins RE, Canfield CJ, Haynes JD, Chulay JD. 1979. Quantitative assessment of
575 antimalarial activity in vitro by a semiautomated microdilution technique. Antimicrob
576 Agents Chemother 16:710-718.
577 40. Smilkstein M, Sriwilaijaroen N, Kelly JX, Wilairat P, Riscoe M. 2004. Simple and
578 inexpensive fluorescence-based technique for high-throughput antimalarial drug screening.
579 Antimicrob Agents Chemother 48:1803-6.
580 41. Haynes JD, Moch JK. 2002. Automated synchronization of *Plasmodium falciparum*
581 parasites by culture in a temperature-cycling incubator. Methods Molec Med 72:489-497.
582 42. Mather MW, Morrisey JM, Vaidya AB. 2010. Hemozoin-free *Plasmodium falciparum*
583 mitochondria for physiological and drug susceptibility studies. Mol Biochem Parasitol
584 174:150-3.
585 43. Olszewski KL, Llinas M. 2013. Extraction of hydrophilic metabolites from *Plasmodium*
586 *falciparum*-infected erythrocytes for metabolomic analysis. Methods Molec Biol 923:259-
587 66.
588 44. Cobbold SA, Chua HH, Nijagal B, Creek DJ, Ralph SA, McConville MJ. 2015. Metabolic
589 dysregulation induced in *Plasmodium falciparum* by dihydroartemisinin and other front
590 line antimalarial drugs. J Infect Dis doi:10.1093/infdis/jiv372.
591 45. Lu W, Clasquin MF, Melamud E, Amador-Noguez D, Caudy AA, Rabinowitz JD. 2010.
592 Metabolomic analysis via reversed-phase ion-pairing liquid chromatography coupled to a
593 stand alone orbitrap mass spectrometer. Anal Chem 82:3212-21.
594 46. Pulcini S, Staines HM, Lee AH, Shafik SH, Bouyer G, Moore CM, Daley DA, Hoke MJ,
595 Altenhofen LM, Painter HJ, Mu J, Ferguson DJ, Llinas M, Martin RE, Fidock DA, Cooper
596 RA, Krishna S. 2015. Mutations in the *Plasmodium falciparum* chloroquine resistance
597 transporter, PfCRT, enlarge the parasite's food vacuole and alter drug sensitivities. Sci Rep
598 5:14552.
599 47. Goecks J, Nekrutenko A, Taylor J, Galaxy T. 2010. Galaxy: a comprehensive approach for
600 supporting accessible, reproducible, and transparent computational research in the life
601 sciences. Genome Biol 11:R86.
602 48. Li H, Durbin R. 2009. Fast and accurate short read alignment with Burrows-Wheeler
603 transform. Bioinformatics 25:1754-60.
604 49. DePristo MA, Banks E, Poplin R, Garimella KV, Maguire JR, Hartl C, Philippakis AA,
605 del Angel G, Rivas MA, Hanna M, McKenna A, Fennell TJ, Kernytsky AM, Sivachenko
606 AY, Cibulskis K, Gabriel SB, Altshuler D, Daly MJ. 2011. A framework for variation

607 discovery and genotyping using next-generation DNA sequencing data. Nat Gen 43:491-
608 8.
609 50. Garrison E, Marth G. 2012. Haplotype-based variant detection from short-read sequencing.
610 arXiv:12073907 [q-bioGN].
611 51. Cingolani P, Platts A, Wang le L, Coon M, Nguyen T, Wang L, Land SJ, Lu X, Ruden
612 DM. 2012. A program for annotating and predicting the effects of single nucleotide
613 polymorphisms, SnpEff: SNPs in the genome of *Drosophila melanogaster* strain w1118;
614 iso-2; iso-3. Fly (Austin) 6:80-92.
615 52. Abyzov A, Urban AE, Snyder M, Gerstein M. 2011. CNVnator: an approach to discover,
616 genotype, and characterize typical and atypical CNVs from family and population genome
617 sequencing. Genome Res 21:974-84.
618 53. Nkrumah LJ, Muhle RA, Moura PA, Ghosh P, Hatfull GF, Jacobs WR, Jr., Fidock DA.
619 2006. Efficient site-specific integration in *Plasmodium falciparum* chromosomes mediated
620 by mycobacteriophage Bxb1 integrase. Nat Methods 3:615-21.
621 54. Fidock DA, Wellems TE. 1997. Transformation with human dihydrofolate reductase
622 renders malaria parasites insensitive to WR99210 but does not affect the intrinsic activity
623 of proguanil. PNAS 94:10931-10936.
624 55. van den Hoff MJ MA, and Lamers WH. 1992. Electroporation in 'intracellular' buffer
625 increases cell survival. Nucleic Acid Res 20:2902.

626

627

628 **Figure Legends:**

629 **Figure 1: Drug-resistant phenotyping of *P.f.* strain SB1-A6.** A) Early ring-stage *P. falciparum*
630 strain D6 (blue) and SB1-A6 (red) were exposed to titrating concentrations of atovaquone or DSM-
631 1. Their susceptibility was directly compared to a phenocopy strain, D10:yDHODH (grey, red
632 outline) and its parent, D10 (grey, blue outline). Parasite survival was determined using a
633 traditional 48-h SYBR-green growth inhibition assay and plotted as an average of three technical
634 replicates (±SD). B) Reversal of the SB1-A6 phenotype is demonstrated by exposure of ring-stage
635 parasites to titrating concentrations of atovaquone with (red circles, dashed line) or without the
636 addition of 1.0 μM proguanil (red circles, solid line). Parasite survival was determined as in (A).
637 C) Whole-cell metabolomic analysis was performed on trophozoite stages of both *P.f.* strain D6
638 and SB1-A6 after two hours of 10x $1C_{50}$ exposure to either atovaquone or DSM-1. Metabolic
639 changes are displayed as a MetaPrint profile (8) and highlighted are the increasing (blue outline)
640 metabolites in D6 compared to no change SB1-A6 (red outline). D) The increased metabolites
641 highlighted (C) in *P.f.* strain D6 (blue) are plotted as absolute signal determined by the average
642 total ion counts (biological duplicates in technical triplicate) for *N*-carbamoyl-L-aspartate and
643 dihydroorotate in the presence of atovaquone (10nM), DSM-1 (1.5 μM) or absence of drug relative
644 to *P.f.* strain SB1-A6 (red).

645

646 **Figure 2: Genetic and molecular differences in *P.f.* strain SB1-A6.** A) Whole-genome
647 sequencing revealed a point mutation in PF3D7_0603300 (*pfdhodh*) and this mutation was verified
648 by Sanger sequencing. A trace of the PfDHODH coding sequence is shown from nucleotide 818-
649 836 and the single nucleotide polymorphism change from the parental D6 to SB1-A6 at nucleotide
650 G827T (yellow highlight) which results in the amino acid change C276F. Additionally, WGS

651 revealed B) a 1.9x copy number increase of a ~20kb region (red highlight) on chromosome 6 which
652 includes PF3D7_0603300 (*pfdhodh*). Copy number increase was calculated and graphically
653 represented using Intansiv (v. 0.99.3). C) Structural comparisons of wild-type (PDB 4RX0, light
654 grey, C276 highlighted in blue) and mutant (PDB 6E0B, dark grey, C276F highlighted in red)
655 PfDHODH bound with FMN, as well as the merged structure surrounding amino acid 276 (inset;
656 cysteine in blue and phenylalanine in red, represent the isosurface of each sidechain) were made
657 using PyMOL 2.3.4. D) Western blot analysis of the PfDHODH expression in both D6 and SB1-
658 A6 probed with anti-mouse PfDHODH antibody (1:300) compared to *Pf*Aldolase (anti-mouse
659 *Pf*Aldolase-HRP, 1:5000) as a loading control. E) Percent inhibition of PfDHODH activity and
660 F) capture of total PfDHODH activity in isolated mitochondria from SB1-A6 (red) and D6 (blue)
661 in the presence of titrating concentrations of DSM-1.

662

663 **Figure 3: Phenotyping Individual Genetic Contributions to *P.f.* SB1-A6 Resistance.** A)
664 Strategy for phenotyping a mimic of the PfDHODH genotype in the wild-type *P.f.* D6 strain.
665 Episomal expression of an additional copy of wild-type PfDHODH (blue) aims to genocopy a
666 CNV and episomal expression of the mutant PfDHODH (red) genocopies a CNV of the mutation
667 to capture the contribution of these genotypes to the resistance phenotype. B) These transgenic
668 lines, D6::wtDHODH (blue triangle, dashed) and D6::mutDHODH (red open circle, dashed), were
669 assessed for their susceptibility to titrating concentrations of both atovaquone and DSM-1 in
670 comparison to the parental strains, A6 (red solid triangle) and D6 (blue solid square). Parasite
671 survival was determined using a traditional 48-h SYBR-green growth inhibition assay and plotted
672 as an average of three technical replicates (±SD). C) Graphic representation of the CRISPR/Cas9-
673 mediated mutational strategy for modification of PfDHODH in both the wild-type D6 and mutant

674 strain SB1-A6. A plasmid expressing Cas9 was cotransfected with a plasmid that contains the
675 DHODH repair template that encodes for C276 (wild-type) or F276 (mutant) that are provided to
676 introduce a single point mutation converting strain D6 to C276F and SB1-A6 to F276C,
677 respectively. The CRISPR/Cas9 mutated strains $D6^{C276F}$ (blue solid diamond, dashed) and SB1-
678 $A6^{F276C}$ (red solid triangle, dashed) were then assayed for their susceptibility to titrating
679 concentrations of both atovaquone and DSM-1 in comparison to the parental strains, A6 (red solid
680 triangle) and D6 (blue solid square). Parasite survival was determined using a traditional 48-h
681 SYBR-green growth inhibition assay and plotted as an average of three technical replicates (±SD).

Figure 1

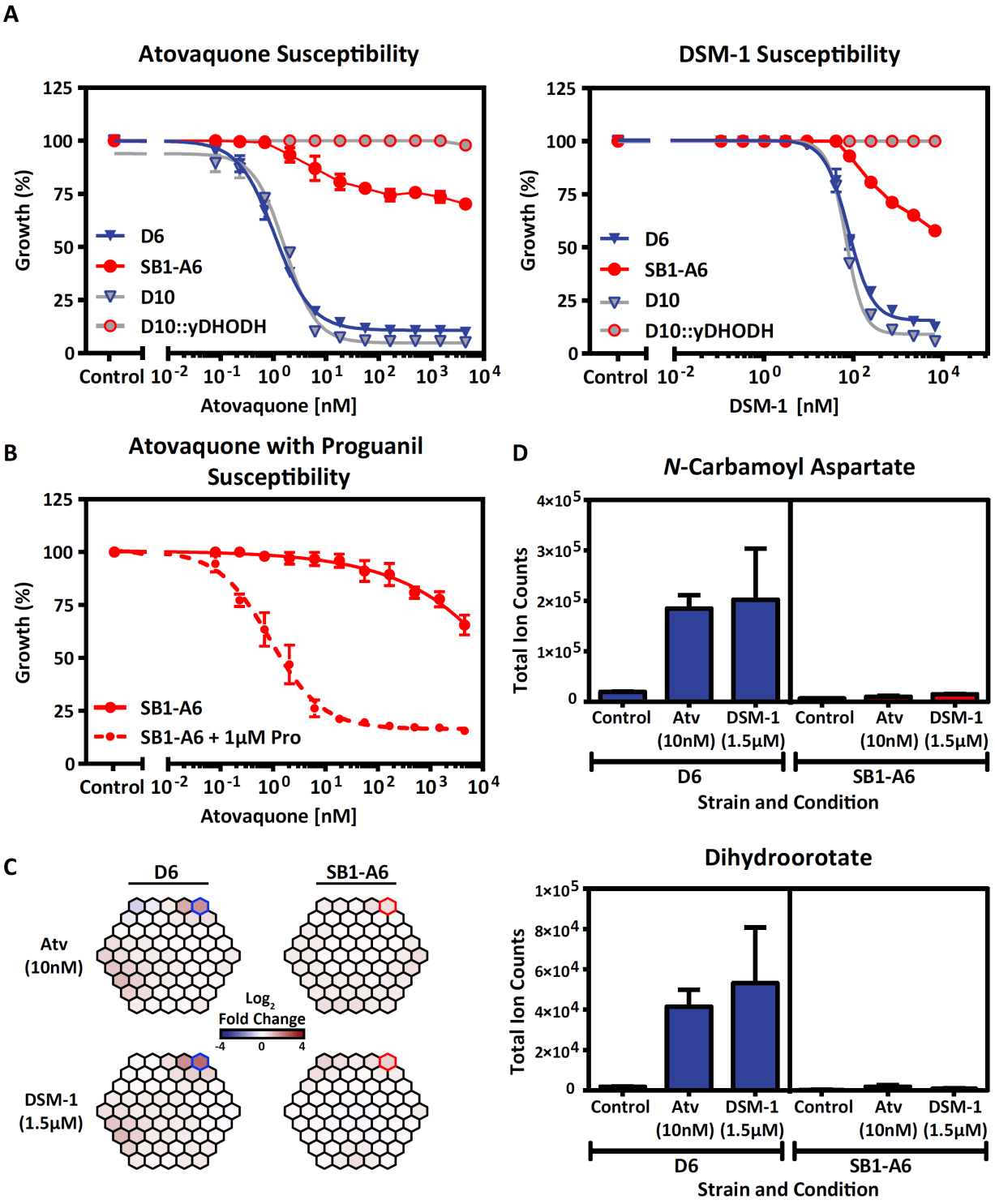

682

683

Figure 2

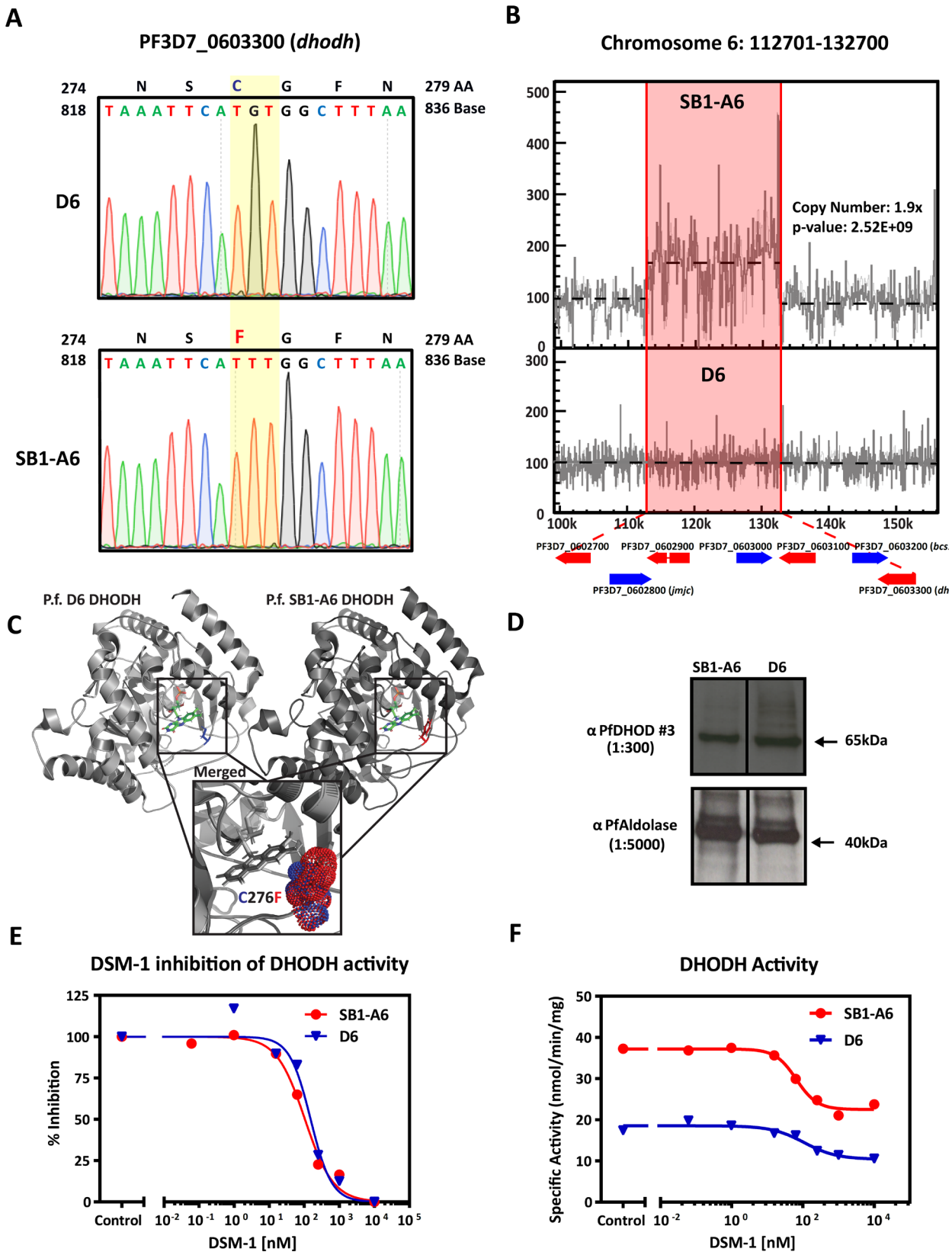
A
PF3D7_0603300 (dhodh)
274 N S C G F N 279 AA
818 T A A A T T C A T G T G G C T T T A A 836 Base
D6
274 N S F G F N 279 AA
818 T A A A T T C A T T T G G C T T T A A 836 Base
SB1-A6
B
Chromosome 6: 112701-132700
SB1-A6
Copy Number: 1.9x
p-value: 2.52E+09
D6
100k 110k 120k 130k 140k 150k
PF3D7_0602700 PF3D7_0602900 PF3D7_0603000 PF3D7_0603100 PF3D7_0603200 (bcs
PF3D7_0602800 (jmjc)
PF3D7_0603300 (dh
C
P.f. D6 DHODH
P.f. SB1-A6 DHODH
Merged
C276F
D
SB1-A6 D6
α PfDHOD #3 (1:300)
65kDa
α PfAldolase (1:5000)
40kDa
E
DSM-1 inhibition of DHODH activity
% Inhibition
SB1-A6
D6
Control 10-2 10-1 100 101 102 103 104 105
DSM-1 [nM]
F
DHODH Activity
Specific Activity (nmol/min/mg)
SB1-A6
D6
Control 10-2 100 102 104
DSM-1 [nM]

684

Figure 3

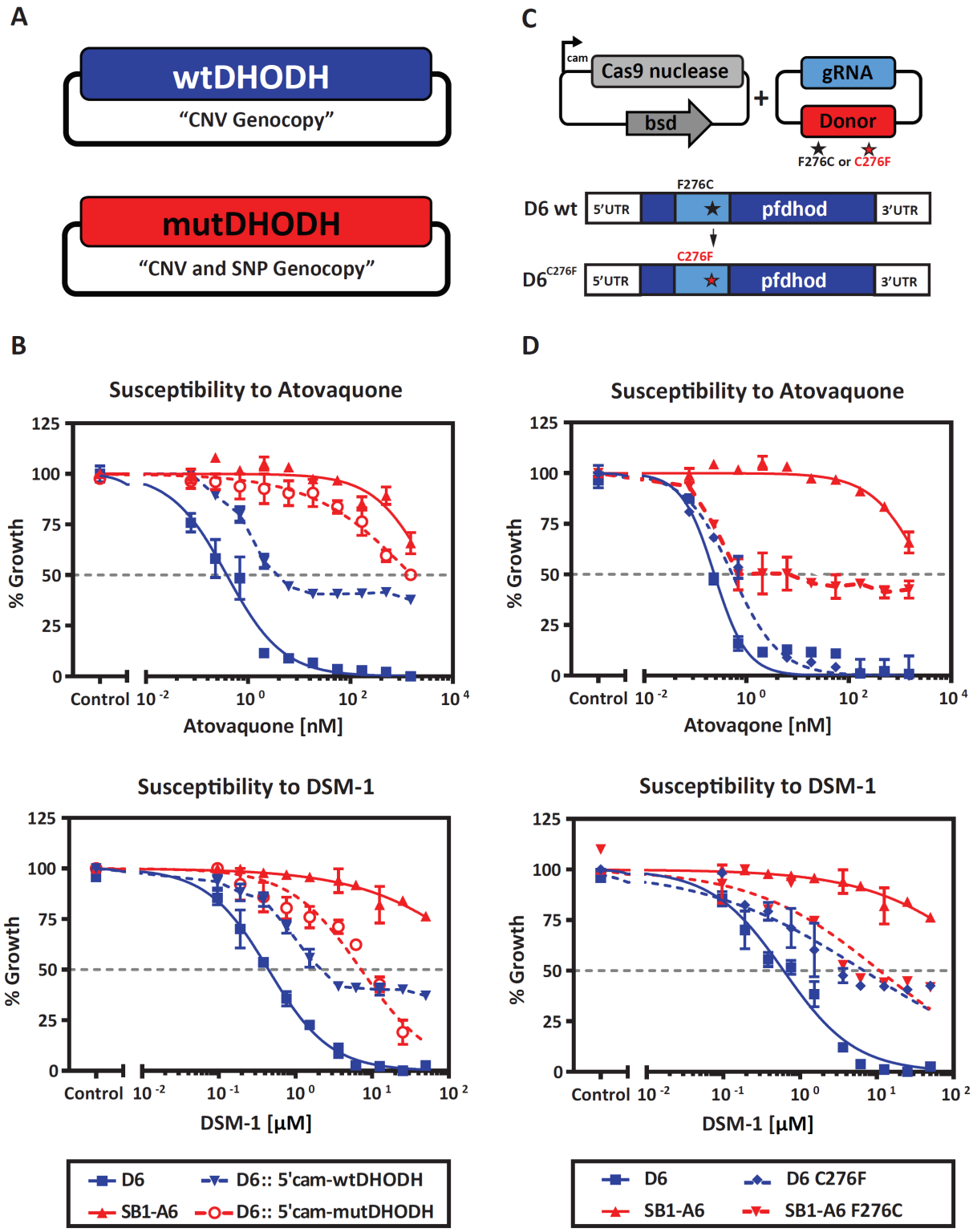

685

686